Journal of Wind Engineering & Industrial Aerodynamics 190 (2019) 112–118

Contents lists available at ScienceDirect

Journal of Wind Engineering & Industrial Aerodynamics

journal homepage: www.elsevier.com/locate/jweia

Climate change impact on typhoon-induced surges and wind field in coastal region of South Korea

Hyeyun Ku [a,*], Jun Ho Maeng [a], Kwangwoo Cho [b]

[a] Div. for Public Infrastructure Assessment, Environmental Assessment Group, Korea Environment Institute, Sejong-si, Republic of Korea
[b] Div. for Integrated Water Management, Water and Land Research Group, Korea Environment Institute, Sejong-si, Republic of Korea

ABSTRACT

Typhoon-induced strong wind is a main factor leading local, weather-related sea-level rise with respect to the global climate change i.e. intensity and frequency of typhoon. This research mainly focuses on obtaining key relations of typhoon-induced wind and surges due to the increase of typhoon intensities. To obtain the winds and surges due to the climate change, this research has employed a dynamic surge model SLOSH (Sea, Lake, and Overland Surges from Hurricanes) which solves two-dimensional Navier-Stokes equations with wind obtained computation of pressure and wind direction for given stationary and circularly-symmetric storm as surface stress. Because of less expensive computational cost, it is suitable model for estimating typhoon-induced wind and surge heights with respect to the highly categorized hypothetical typhoons due to global warming. The hypothetical typhoons are composed by increasing mean sea level pressure (MSLP) and choosing corresponding radius of maximum wind (RMW) along a path of historical typhoon MAEMI (2003). The increment of MSLP resulted in the decrease of the maximum wind speed by same decline rations without dependence on the local characteristics. However, the typhoon-induced surge heights are strongly depending on the typhoon intensity and the local bathymetry. In addition, a comparison of numerically estimated wind to observational data resulted in ±50% error bounds which are corresponding to residuals appeared in the typhoon-induced surge heights.

1. Introduction

Typhoon-induced surge (also called as storm surge) is an abnormal sea level rise of water above the astronomical tide generated by typhoon-induced strong winds blowing over shallow and continental shelves. This local, meteorological surge is one of components causing sea-level rise and this leads coastal inundation by pushing the water to the coast. Along with global warming effect, increase of global energy which can shift the intensity of tropical cyclones to the stronger storms can result in extreme weather-related hazards such as the typhoon-induced stronger winds, the locally weather-related sea-level rise, and further the coastal inundation (Li et al. (2015), Mudd et al. (2014), Oh and Moon (2013), Knutson et al. (2010), IPCC, (2013)). In addition, in Korean coastal area, high risks to the coastal weather-related disasters are increasing by growing population and urbanization (Weather Meteorological Organization (2017), Kang et al. (2018)).

According to studies on projection of tropical cyclones in accordance with global warming, in the western North Pacific, a number of tropical cyclones is decreasing, but frequency of intense tropical cyclones, in particular 3–4 categories hurricanes of Saffir-Simpson Hurricane Damage-potential scale, is increasing (Knutson and Tuleya (2004), Murakami, et al. (2011), Murakima et al., 2012, Song et al. (2010); Walsh et al. (2016); Ying et al. (2012); Yoshida et al. (2017); Ahren (2004)). The greenhouse effect leads higher frequency of those intense typhoons by heating the ocean surface and supplying energy to develop the high category tropical cyclones. It is obvious that those intense typhoons have resulted in vast damages in human society and economics. These climate change impacts on the occurrence of the stronger typhoons and further potential damages motivate studying the effect of typhoon intensity on the typhoon-induced winds and surges as a first step forward the coastal inundation due to the both global and local, weather-related sea-level rise in accordance to the climate change.

On estimating the wind speed for some weather-related hazard risk projects such as assessing hurricane risk and developing structure standard, mathematical simulations have been widely used (Vickery et al. (2009); Lee et al. (2015)). Here in this research, the typhoon-induced winds and surges can be calculated with less expensive computational cost by employing the model SLOSH (Sea, Lake, and Overland Surges from Hurricanes) which was developed by National Oceanic and Atmospheric Administration (NOAA), an agency of the U.S. department, with a purpose of forecasting storm surge heights (Jelesnianski et al. (1984, 1992), Shaffer et al. (1989), Taylor and Glah (2008), Glahn et al. (2009) and Lee et al. (2015)). Even though the model SLOSH considers only meteorological effect and has up to ±20% to ±50% error bounds on seas

* Corresponding author.
E-mail addresses: hyku@kei.re.kr, hyeyun.ku@gmail.com (H. Ku).

https://doi.org/10.1016/j.jweia.2019.04.018
Received 30 September 2018; Received in revised form 19 April 2019; Accepted 19 April 2019

0167-6105/© 2019 Elsevier Ltd. All rights reserved.

of Korea (Ku et al. (2019) and Seo et al. (2018)), these disadvantage are overcome by adopting probabilistic approach with respect to various hypothetical typhoons (Taylor and Glah (2008)). The hypothetical typhoons can be established by adopting Monte-Carlo Simulation (MCS) which estimates typhoon path, mean sea level pressures at typhoon center, and radius of maximum winds (Lee (2010); Kim and Suh (2018)). To consider the climate change effect onto those hypothetical typhoons, this study have chosen various mean sea level pressures, according to some simulation and projection results from Knutson and Tuleya (2004), Murakami, et al. (2011), Murakima et al., 2012, Song et al. (2010), Walsh et al. (2016), Ying et al. (2012), and Yoshida et al. (2017). Those proposed an assumption on potential changes as many as possible on the path, intensity and genesis frequencies, with particular to the increase of high-scaled typhoon genesis as like as 3–4 Saffir-Simpson hurricane categories.

An ultimate goal of this research is obtaining key insight on climate change impact on variation of typhoon-induced surges with respect to typhoon intensity, with particular on the typhoon-induced strong winds, in the coastal region of South Korea by adopting the deterministic model SLOSH. This model SLOSH was already validated on the estimation of typhoon-induced surge heights around Korean coast (Ku et al. (2019); Seo et al. (2018)). As the surge becomes higher, the error have decreased to ±20% (Ku et al. (2019); Seo et al. (2018); Glahn et al. (2009)). Based on these validations, there is a possibility of using the wind module of SLOSH to achieve the research goal. Firstly, to clarify applicability of the model SLOSH on estimating both wind field and surge heights, the numerically estimated wind field of the historical typhoon MAEMI (2003) is compared with observational data at two tidal stations; Masan and Tongyeong. Then, considering the climate change impact, a total of 8 hypothetical typhoons are adopted based on the path of typhoon MAEMI (2003). Mean sea level pressure (MSLP) and radius of maximum wind (RMW) are set in a range of 3–4 Saffir-Simpson hurricane categories. The SLOSH results on typhoon-induced winds and surges are compared with respect to the typhoon intensity.

2. Methodology

SLOSH (Sea, Lake, and Overland Surges from Hurricanes).

To estimate the meteorological sea-level rise by typhoon, SLOSH (Sea, lake, and Overland Surges from Hurricanes), a deterministic model forecasting typhoon-induced surge heights is adopted. The model SLOSH was developed with a purpose of forecasting the real-time storm surges and establishing evacuation plan for hurricane on the coastal area by National Oceanic and Atmospheric Administration (NOAA), an agency of the U.S. Department. It is noted that the governing equations employed in the model SLOSH are written as given in recent study which applied the model SLOSH for seas of Korea (Ku et al. (2019), Seo et al. (2018)).

SLOSH is mainly consisting of two models; wind and storm surge. The wind model computes the pressure and wind direction for a stationary and circularly-symmetric storm which is given as a data set of longitudinal and latitudinal position of the typhoon center, central pressure, maximum wind speed, and radius of the maximum wind speed. The model is given by (Jelesnianski et al. (1992); Kim et al. (1996); Jelesnianski and Taylor (1973))

$$\frac{1}{\rho_a}\frac{dp(r_t)}{dr_t} = \frac{k_s V^2}{\sin\phi} - V\frac{dV}{dr_t} \tag{1}$$

$$\frac{1}{\rho_a}\frac{dp}{dr_t}\cos\phi = fV + \frac{V^2}{r_t}\cos\phi - V^2\frac{d\phi}{dr_t}\sin\phi + k_n V^2 \tag{2}$$

when the wind speed profile is given by

$$V(r_t) = V_R\frac{2Rr_t}{R^2 + {r_t}^2}. \tag{3}$$

r_t is the distance from the storm center to any given location within the circularly-symmetric storm, $p(r_t)$ is the pressure, $\phi(r_t)$ is the inflow angle across circular isobars toward the storm center, and $V(r_t)$ is the wind speed. k_s and k_n are empirical coefficients for surface friction. R is the radius of maximum wind and V_R is the maximum wind speed. This wind profile for the stationary storm is corrected by empirical formulation which is tapered off to zero at $r_t = 0$ and $r_t = \infty$. Only moderate to extreme typhoons created the little typhoon-induced surges. However, it is less important since the typhoon-induced surge model is not sensitive to the surge heights induced by wind from the movement of the typhoons.

The surge model derives the typhoon-induce surge heights by solving shallow water equations which was transformed in conformal from $z = (x, y)$ to $\varsigma = (P, Q)$ and is then particularized onto a polar frame of reference given by (see Jelesnianski et al. (1992); Kim et al. (1996))

$$\zeta = P + iQ = \ln\left(\frac{r}{R_o}\right) + i\theta, \tag{4}$$

where R_o is a convenient scale. The final form of the transport equations is given by

$$\frac{\partial U}{\partial t} = -g(D+h)\left[B_r\frac{\partial h}{\partial P} - B_i\frac{\partial h}{\partial Q}\right] + f(A_r V + A_i U) + r[\cos\theta X_T + \sin\theta Y_T], \tag{5}$$

$$\frac{\partial V}{\partial t} = -g(D+h)\left[B_r\frac{\partial h}{\partial Q} + B_i\frac{\partial h}{\partial P}\right] + f(A_r U + A_i V) + r[\cos\theta Y_T - \sin\theta X_T],$$

subject to

$$\frac{\partial h}{\partial t} = -\frac{1}{r^2}\left(\frac{\partial U}{\partial P} + \frac{\partial V}{\partial Q}\right). \tag{6}$$

The atmospheric forcing terms T_x and T_y are defined on the Cartesian coordinate system (x, y)

$$T_x = g(D+h)\left(B_r\frac{\partial h_0}{\partial x} - B_i\frac{\partial h_0}{\partial y}\right) + C_r\tau_x - C_i\tau_y, \tag{7}$$

$$T_y = g(D+h)\left(B_r\frac{\partial h_0}{\partial y} - B_i\frac{\partial h_0}{\partial x}\right) + C_r\tau_y - C_i\tau_x. \tag{8}$$

U and V are components of volume transport on the polar frame of reference, D is depth of quiescent water relative to a common datum, h is a height of water above the reference datum, h_0 is a hydrostatic water height, f is a Coriolis parameter, τ_x and τ_y are components of surface stress, and A_r A_i, B_r, B_i, C_r, and C_i are bottom stress coefficients with scripts of r and i for real and imaginary, respectively. The surface stresses over water bodies are from the meteorological source, i.e. wind, by converting the wind given in Equations (1)–(3) to the one at usually 10 m heights above the sea. These transport equations are numerically are marched two or three level forward in time and central differencing in space.

2.1. Validation and statistical assessment

To validate the wind model, the historical typhoon MAEMI (2003) has chosen because of its strong winds pushed lots of ocean water to the southern coastal cities such as Masan and Tongyeong. The two tidal stations, Masan and Tongyeong, are used as points for validating the wind model and further seeing trends of weather-related winds and surges in accordance with the climate change (see Fig. 1(a)). Briefly explaining the typhoon MAEMI (2003), as shown in Fig. 1, it had passed through the southern coast of Korea around Sep 12, 2003(KST). Meanwhile, it was developed up to 3rd scaled typhoon in Saffir-Simpson Hurricane Damage-potential scale (Ahren (2004)). When it has approached to the land, the mean sea level pressure (MSLP) had reached

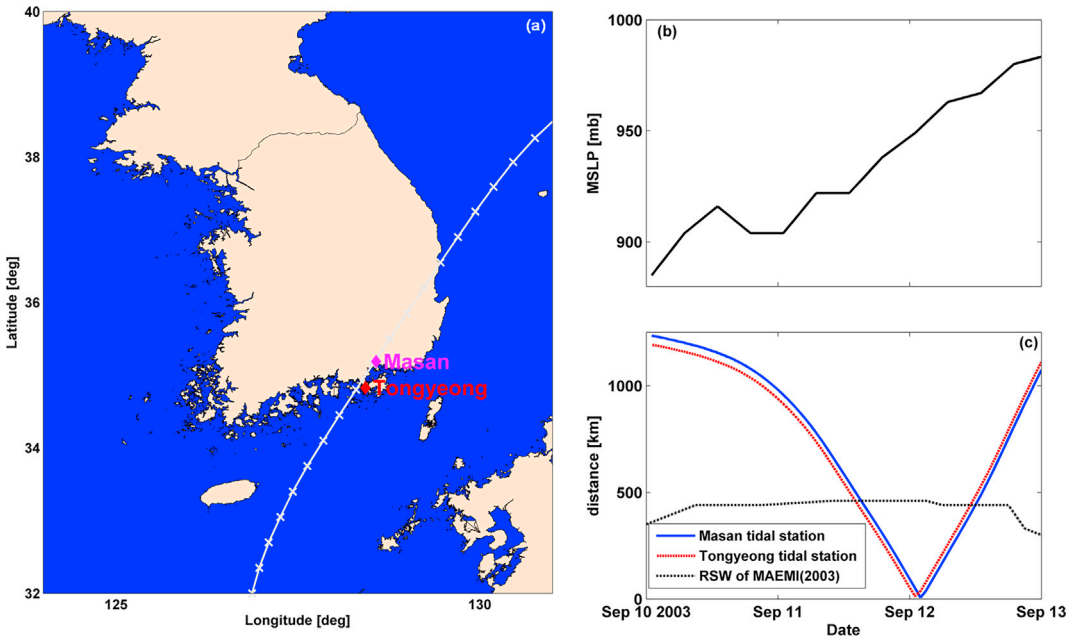

Fig. 1. Typhoon MAEMI (2003). (a) Track (white straight line with X-marker) and locations of Masan (magenta diamond) and Tongyeong (red diamond) tidal stations, (b) time-varying mean sea level pressure (MSLP) and (c) distances between the typhoon center and the tidal stations from Sep 10, 2003 to Sep 12, 2003.

to approximately 950 mb (Fig. 1(b)). Considering that the most typhoons were landed after they weakened to tropical cyclones, its scale was comparatively strong. Fig. 1(c) shows how closely the typhoon passed two tidal stations (see blue straight line for Masan tidal station and red dashed line for Tongyeong one). A black dashed-dot line shows radius of strong wind (RSW) which is consisting of isotach of $15\,\mathrm{m\,s^{-1}}$ typhoon-induced wind from the typhoon center. While the typhoon MAEMI is passing over those two tidal stations, the RWS was approximately 440–460 km and the radius of maximum wind (RMW) was about 55.6 km.

The time-varying wind speeds from the model SLOSH is compared to observational data of Korea Meteorological Administration (KMA). KMA provides minutely and hourly wind speed data while the SLOSH wind model calculates instantaneous wind speed at each time-step. To match those wind averaged on different periods, we have adopted gust factors obtained by empirical relation from researches of Durst (1960) and Cao et al. (2015). The gust factors converting hourly mean wind speed to wind speed of shorter period such as 0.5 s, 1 s, 3sec and minutely probable periods are ranges from approximately 1.2 to 1.6. Also, Cao et al. (2015) have showed no significant differences on typhoon gust factors with respect to the winds which is associated with typhoon or not through a cast study on gust factor of the strong typhoon MAEMI (2003). This research has adopted their gust factors with respect to mean wind speed so that some coefficients suitable for the range of observational wind speeds have been chosen to correct the KMA wind speed. Note that since the KMA wind speed was observed above 10 m from the earth and the SLOSH wind field is calculated 10 m above the water or land surfaces. Also, the locations of KMA synoptic weather observation are very close to the coast and the both tidal stations so that it is the observational winds are corrected only with respect to the observational periods.

Differences of the numerically estimated and the corrected KMA observational wind speeds are quantified by calculating root-mean-square error (RMSE) and a coefficient of determination r^2 as follows

$$\mathrm{RMSE} = \sqrt{\frac{1}{n}\sum_{i=1}^{n} e_i^2}, \tag{9}$$

$$r^2 = \frac{SS(Regr)}{SS(Regr) + SS(Res)}, \tag{10}$$

where $e_i = x_{OBS,i} - x_{SLOSH,i}$ is a residual between $x_{OBS,i}$ and $x_{SLOSH,i}$ and those are typhoon-induced storm surge heights at i-th time step obtained from KMA and SLOSH, respectively. $SS()$ means of sum squares with respect regression ($Regr$) and residual (Res) following Rawlings et al. (1998). Each is defined as $SS(Res) = \sum_{i=1}^{n} e_i^2$ and $SS(Regr) = \sum_{i=1}^{n} (x_{OBS,i} - \overline{x_{OBS}})^2$. Those statistical coefficients show how the numerically estimated values are closely predicted to the observational ones.

2.2. Problem configuration

As mentioned in the above, the previous simulations and projections have agreed that the occurrence frequency of tropical cyclones on the western North Pacific is decreasing meanwhile the number of intense typhoon is increasing due to the climate change (Knutson and Tuleya (2004); Murakami et al. (2011), Murakima et al., 2012; Walsh et al. (2016); Oh and Moon (2013); Ying et al. (2012); Yoon et al. (2012)). Particularly, Especially, Knutson and Tuleya (2004) resulted in higher occurrence of typhoons of categories 3–4 of the Saffir-Simpson hurricane intensity scale for both controlled and high CO_2 cases. Mean sea level pressures (MSLP) of such intensive hurricanes are ranges from 920 to 964 (Ahren (2004)). Those values are corresponding to minimum values for 50- and 100-years return period obtained from distribution of extreme values based on historical typhoons affected on Korean peninsula from 1970 to 2010. As follows the Saffir-Simpson hurricane intensity scale, we chose various MSLP to consider the climate change and the variations are listed in Table 1. The minimum MSLP is set as the smallest one while the typhoon is in developing status and the landed MSLP is the value when the typhoon is landed in the southern coast of Korea. Since the typhoons have been weakening while they were passing around Korea, it is applied for the hypothetical typhoons as shown in two MSLPs of Table 1. Note again that the typhoon is moving as same as path of the typhoon MAEMI (2003).

Table 1
Simulation cases and maximum wind speed obtained from observation at Masan and Tongyeong tidal stations and the wind model in the model SLOSH.

Case No.			MAEMI	1	2	3	4	5	6	7	8
MSLP [mb]	Min.		910.0	933.0	902.0	943.0	912.0	955.0	936.0	962.5	941.0
	Landed		949.0	942.0	950.0	952.0	960.0	970.0	972.0	975.0	977.0
Max.Wind Speed [m s^{-1}]	Masan	Obs.	28.20	–	–	–	–	–	–	–	–
	Tongyeong	SLOSH	36.80	46.27	41.64	41.12	37.58	32.57	31.46	30.14	29.34
	Masan	Obs.	45.43	–	–	–	–	–	–	–	–
	Tongyeong	SLOSH	42.09	47.37	43.51	42.85	38.59	33.66	32.56	31.03	30.19

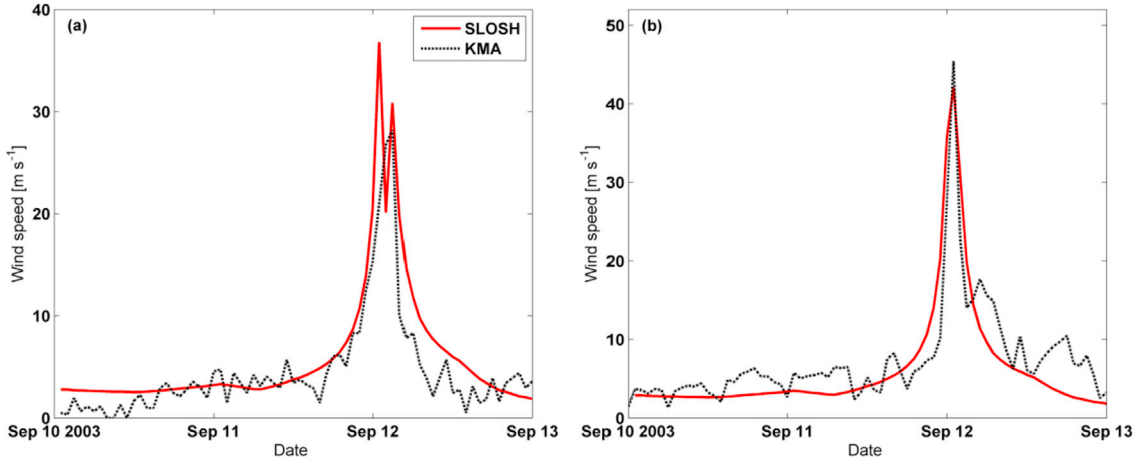

Fig. 2. Comparison of time-varying wind from SLOSH (red straight line) and KMA (black dash-dotted line) at (a) Masan tidal station and (b) Tongyeong tidal station.

3. Result

3.1. Wind field validation

Fig. 2 shows the time-varying winds induced by the typhoon MAEMI at (a) Masan and (b) Tongyeong tidal stations. As the typhoon MAEMI is approaching to the southern coast of Korea, i.e. the distances from the typhoon center to the tidal stations are getting shorter as shown in Fig. 1(c), the wind speed increasing. Particularly, the values are dramatically increasing when the tidal stations are facing the approaching typhoon and those are located within the symmetric radius of 15 m s^{-1} isotaches of the typhoon-induced winds. This radius of strong wind is approximately 440–460 km according to KMA (see Fig. 1(c)). Soon after the typhoon has passed through the stations so that those tidal stations are located rear side of the typhoon, the wind speeds are dramatically decreased even though the stations are within the RSW. It resulted from no heat energy supply from the ocean after the typhoon has landed. In Fig. 2, it seems that the wind module of the model SLOSH follows the KMA wind pattern at both tidal stations, however, there are two peaks on the SLOSH winds at Masan tidal station. There are two possibilities: (1) the typhoon MAEMI (2003) had passed nearby the Masan tidal station so that the tidal station was located within the radius of max wind where the wind is decreasing toward the typhoon (see Equation (3) for detail), and (2) the balance of forces in the gyrating storm gives the secondary maxima (Jelesnianski and Taylor (1973)).

Comparing the maximum values, the wind speeds are over- and under-estimated by 8.6 m s^{-1} and 3.43 m s^{-1} at Masan and Tongyeong tidal stations, respectively (see Table 1 for details). The model SLOSH estimated the maximum wind earlier than the observation. Their phase errors are approximately 2 h, but the SLOSH wind model estimated relatively high wind at the maximum KMA wind data. These resulted in the smaller RMSE and the quietly higher coefficient of the determination r^2. The RMSE values are 3.18 and 3.51 at Masan and Tongyeong tidal stations, respectively. The determination coefficient is 0.80 for both tidal stations as shown in Table 2. These values are computed based on the one-to-one correspondence of the SLOSH wind speed to the KMA data

Table 2
Root-mean square error (RMSE) and coefficient of determination r^2.

Tidal station	RMSE	r^2
Masan	3.18	0.80
Tongyeong	3.51	0.80

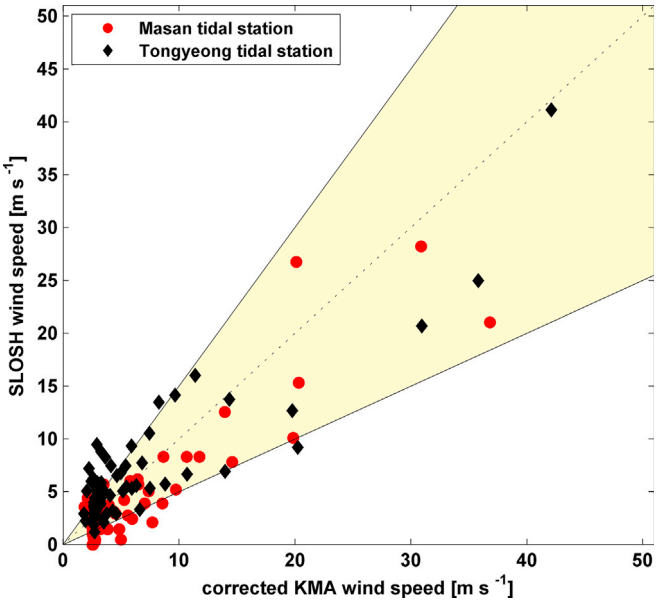

Fig. 3. Comparison of corrected KMA wind speeds and the SLOSH results.

shown in Fig. 3. At relatively high wind, e.g. greater than 10 m s^{-1}, the difference becomes larger up to about 15.8 m s^{-1} at Masan tidal station. This difference is within the error bound of ±50% which is yellow area in Fig. 3. Analogous with large error bound for the relatively lower surge heights less than 3 m (Glahn et al., 2009), this ±50% in the SLOSH wind

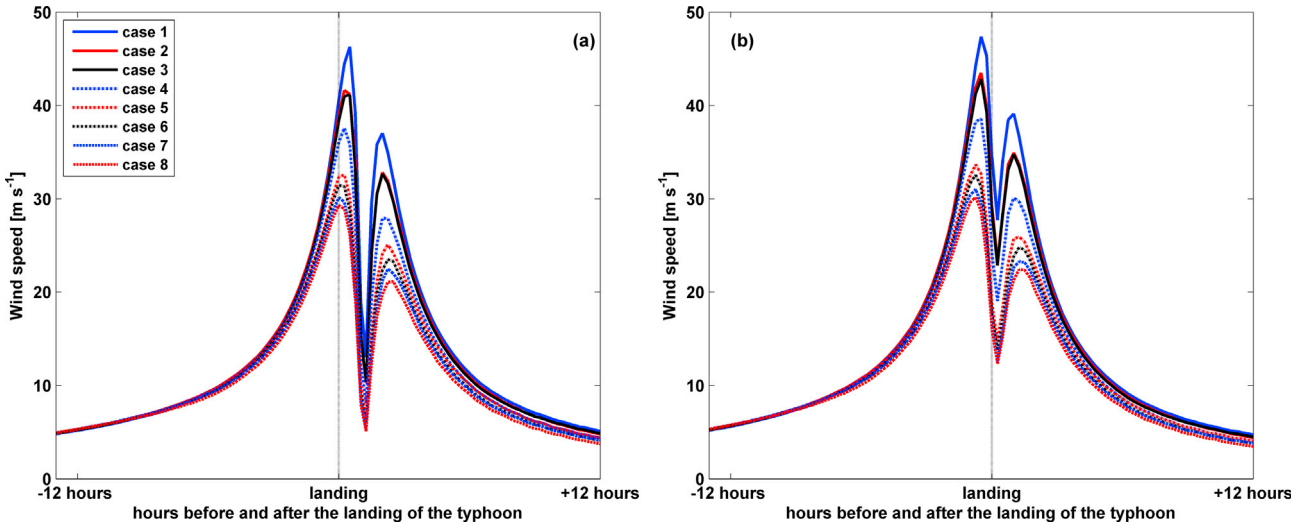

Fig. 4. SLOSH wind speed before to after 12 h from typhoon landing at (a) Masan and (b) Tongyoeng tidal stations.

model is acceptable. It can be seen that the typhoon-induced surge heights varying within the error bound as same as the wind in the previous studies of Ku et al. (2019) and Seo et al. (2018) are subsequence of the wind model on calculating the surge heights in the model SLOSH.

3.2. Climate change impact on typhoon-induced wind field and surges

Fig. 4 shows numerically estimated time-varying wind. For all cases, the wind speeds reached to the maximum values around the landing of the hypothetical typhoons which had developed by the different minimum MSLP as given in Table 1 on the same path of the typhoon MAEMI (2003). Both tidal stations are within the radius of strong wind of 15 m s^{-1} for almost 24 h while the typhoon is passing through the southern coast of Korea. While the tidal stations are facing the approaching typhoon within the radius of strong wind (RSW), the wind speed is increasing. Soon after the tidal stations are within the radius of maximum wind (RMW), i.e. the typhoon center has approached very close to the tidal station; the wind speed is rapidly decreased. When those stations are out of the RMW, the wind has increased again and the third inflection points are appeared. Each curve has three inflection points; 2 maximum and 1 minimum. Those maximums and minimum values are decreasing with respect to the increment of the minimum MSLP. Also, the differences between the inflection points are getting smaller at higher MSLP.

The higher wind stress corresponding to the lower mean surface pressure level definitely resulted in higher surge heights as shown in Fig. 5. At both tidal stations, the maximum surge heights have occurred when the typhoon is closely approaching toward the tidal stations. The following dramatic decrease of the wind resulted in sudden drop of the surge heights. While those are converging to the stationary state, i.e. 0 m, the typhoon-induced surge heights oscillated in a shape of under-damping motion. Even though there was the third inflection point in the wind profile (Fig. 4), those were not acted as forces raising the sea level. The vectorized wind field onto the $r-\theta$ coordinate cancelled out the wind at southern part of the typhoon which is moving toward to the next place. As shown in Fig. 1, the tidal stations are located in the rear of the moving typhoon i.e. when it passed them, the effect of the higher wind was cancelled, and the surge heights were not raised. Comparing the maximum typhoon-induced surge heights at two tidal stations with respect to the maximum wind speeds, the Tongyeong tidal station have less surge heights by approximately 1 m than Masan station. It can be

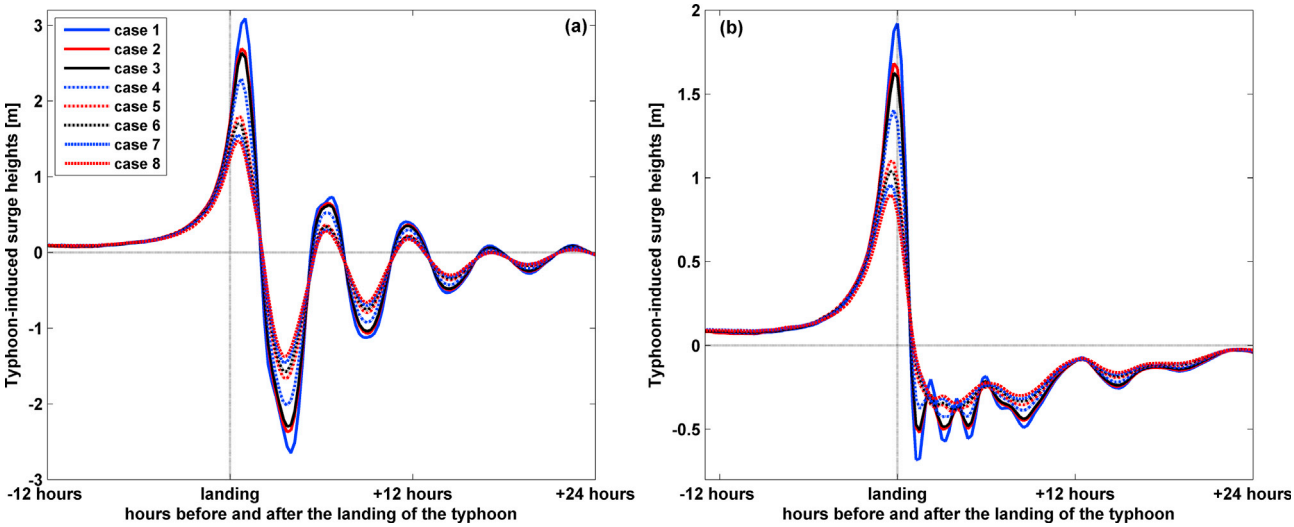

Fig. 5. SLOSH typhoon-induced surges for 72 h at (a) Masan and (b) Tongyeong tidal stations.

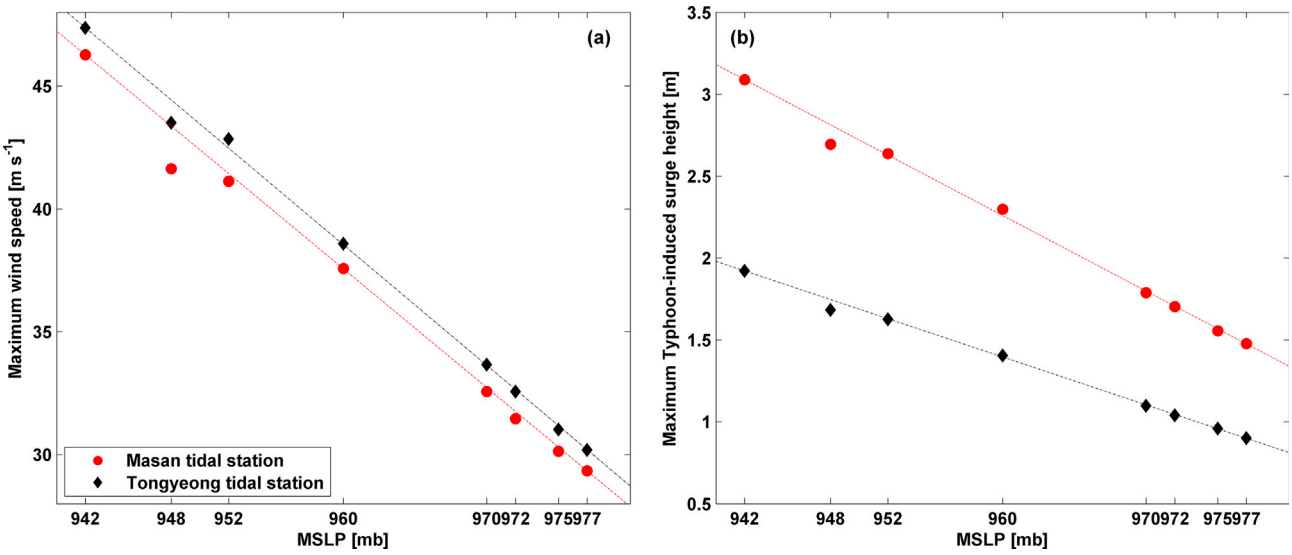

Fig. 6. Maximum values with respect to the mean sea level pressure (MSLP) (a) wind speed and (b) typhoon-induced surge heights.

expected that local characteristics of Masan bay that is long and narrow channel from the ocean and it develops and amplify the surface waves along the channel, resulted in the less surge heights.

Fig. 6 (a) and (b) show one-to-one correspondence of maximum wind speed and typhoon-induced surge heights to the intensity of typhoon i.e. mean sea level pressure (MSLP) on land, respectively. At the two tidal stations, the maximum wind speeds are linearly decreasing as the intensity is decreasing with a ratio of approximately −0.5. The maximum typhoon-induced surge heights are also linearly decreasing, but their ratio is depending on the location of the tidal stations. At Masan tidal station, amplitude is decreased from about 3 m to 1.5 m with respect to the increment of the MSLP from 942 mb to 977mb. Its decreasing ratio is −0.046. At Tongyeong tidal station, the maximum surge heights are decreased by a ratio of −0.029. Also, the higher wind speed at the Tongyeong tidal station than Masan has not led the higher typhoon-induced surges. In case of Masan tidal station, it is located in Masan bay which is long enough to propagate wave from the ocean to the coast. It can be seen that the local characteristics quietly, strongly affected on the surge heights.

4. Conclusion

On the estimation of wind fields and surge heights, the category of typhoon which is scaled up with respect to climate change, i.e. increase of sea surface temperature due to global warming, is important parameter since it can be connected with increase of typhoon intensity and further typhoon-induced wind and surge heights. This study estimated the wind speed and the typhoon-induced surge heights under hypothetical typhoons which are included in 3–4 categories of Saffir-Simpson intensity scales. Firstly, the wind speed which is calculated as a function of distance from the storm center r_t and the maximum wind speed V_r as shown in Equation (3) which is linearly proportional to the typhoon intensity, the increment of the MSLP with a decline ratio of −0.5. Whereas, the typhoon-induced surge heights decreasing as the MSLP is increasing. Their decline is strongly dependent on the local characteristics such as bathymetry.

Also, the wind field validation have led the error-bounds up to ±50%. It can be seen that those error should be considered in estimation of typhoon-induced surge heights because the surface stress over the sea is proportional to the wind speeds. To obtain key insight on estimating climate change impact on the typhoon-induced surge heights and using in the study on the estimating coastal inundation, it requires obtaining more relationship between MSLP, wind speed and the typhoon-induced surge height for potentially available hypothetical, intense typhoons with respect to the climate change.

Acknowledgements

This study was funded by the Korea Ministry of Environment (MOE) as “Climate Change Correspondence Program(2014001310006).”

References

Ahren, C.D., 2004. Essentials of Meteorology, fourth ed. Brooks/Cole Publishing Co., p. p311

Cao, S., Tamura, Y., Kikuchi, N., Saito, M., Nakayama, I., Matsuzaki, Y., 2015. A case study of gust factor of a strong typhoon. J. Wind Eng. Ind. Aerod. 138, 52–60.

Durst, C.S., 1960. Wind speeds over short periods of time. Meteorol. Mag. 89–1056, p181–186.

Glahn, B., Taylor, A., Kurkowski, N., Shaffer, W.A., 2009. The role of the SLOSH model in national weather service storm surge forecasting. Natl. Weather Digest 33–1, p3–14.

IPCC, 2013. In: Stocker, T.F., Qin, D., Plattner, G.-K., Tignor, M., Allen, S.K., Boschung, J., Nauels, A., Xia, Y., Bex, V., Midgley, P.M. (Eds.), Climate Change 2013: the Physical Science Basis. Contribution of Working Group I to the Fifth Assessment Report of the Intergovernmental Panel on Climate Change. Cambridge University Press, Cambridge, United Kingdom and New York, NY, USA.

Jelesnianski, C.P., Taylor, A.D., 1973. A preliminary view of storm surges before and after storm modifications. In: NOAA Technical Memorandum ERL WMPO-3. Weather Modification Program Office, Boulder, Colorado, USA.

Jelesnianski, C.P., Chen, J., Shaffer, W.A., Gilad, A.J., 1984. SLOSH – a Hurricane storm surge forecast model. Oceans p314–317.

Jelesnianski, C.P., Checn, J., Shaffer, W.A., 1992. SLOSH: sea, lake, and Overland surges from hurricanes. In: NOAA Technical Report NWS 48. National Weather Service, Silver Spring, M.D. USA.

Kang, T.S., Oh, H.M., Lee, E.I., Jeong, K.Y., 2018. Disaster vulnerability assessment in coastal areas of Korea. J. Coast. Res. SI 85, p886–890. https://doi.org/10.2112/SI85-178.1.

Kim, H.-J., Suh, S.-W., 2018. Improved hypothetical typhoon generation technique for storm surge frequency analyses on the Southwest Korean coast. J. Coast. Res. SI 85, p516–520. https://doi.org/10.2112/SI85-104.1.

Kim, S.-C., Chen, J., Shaffer, W.A., 1996. An operational forecast model for extratropical storm surges along the U.S. East Coast. Preprints, Conference on Oceanic and atmospheric Prediction, Atlanta, Georgia, USA. Amer. Meteor. Soc. p281–286.

Knutson, T.R., Tuleya, R.E., 2004. Impact of CO_2-induced warming on simulated hurricane intensity and precipitation: sensitivity to the choice of climate model and convective parameterization. J. Clim. 17–18, p3477–3495. <3477:IOCWOS>2.0.CO;2. https://doi.org/10.1175/1520-0442(2004)017.

Knutson, T.R., McBride, J.L., Chan, J., Emanuel, K., Holland, G., Landsea, C., Held, I., Kossin, J.P., Srivastava, A.K., Sugi, Masato, 2010. Tropical cyclones and climate change. Nat. Geosci. 3, p157–163. https://doi.org/10.1038/ngeo779.

Ku, H., Maeng, J.H., Cho, K., 2019. Deterministic estimation of typhoon-induced surges and inundation on Korean coastal regions. J. Korean Soc. Coast. Ocean Eng. 31–1, 1–8. https://doi.org/10.9765/KSCOE.2019.31.1.1.

Lee, S., Won, C.H., Park, H.K., 2015. Stochastic estimation of storm surge height in Gyeonggi-bay. J. Wind Eng. Inst. Kor. 18–4, p163–170.

Lee, Y.-K., 2010. Development of Model for Wind Hazard Assessment Based on Geographical Information. ChungBuk National University, pp. p74–87.

Li, L., Kareem, A., Xiao, Y., Song, L., Zhou, C., 2015. A comparative study of field measurements of the turbulence characteristics of typhoon and hurricane winds. J. Wind Eng. Ind. Aerod. 140, 49–66. https://doi.org/10.1016/j.jweia.2014.12.008.

Mudd, L., Wang, Y., Letchford, C., Rosowsky, D., 2014. Hurricane wind hazard assessment for a rapidly warming climate scenario. J. Wind Eng. Ind. Aerod. 133, 242–249. https://doi.org/10.1016/j.jweia.2014.07.005.

Murakami, H., Wang, B., Kitoh, A., 2011. Future change of western North Pacific typhoons: projections by a 20-km-Mesh global atmospheirc model. J. Clim. 24, p1154–1169. https://doi.org/10.1175/2010JCLI3723.1.

Murakima, H., Wang, Y., Yoshimura, H., Mizuta, R., Sugi, M., 2012. Future changes in tropical cyclone activity projected by the new high-resolution MRI-AGCM. J. Clim. 25, p3231–3260. https://doi.org/10.1175/JCLI-D-11-00415.1.

Oh, S.M., Moon, I.-J., 2013. Typhoon and storm surge intensity changes in a warming climate around the Korean Peninsula. Nat. Hazards 66–3, 1405–1429. https://doi.org/10.1007/s11069-012-0422-z.

Rawlings, J.O., Pantula, S.G., Dickey, D.A., 1998. Applied Regression Analysis: a Research Tool, second ed. Springer-Verlag New York, Inc., New York, USA.

Seo, J., Ku, H., Cho, K., Maeng, J.H., Lee, H., 2018. Application of SLOSH in estimation of typhoon-induced storm surges in the coastal region of South Korea. J. Coast. Res. SI 85, p551–555. https://doi.org/10.2112/SI85-111.1.

Song, J.-J., Wang, Y., Wu, L., 2010. Trend discrepancies among three best track data sets of western North Pacific tropical cyclones. J. Geophys. Res. 115, D12128. https://doi.org/10.1029/2099JD013058.

Shaffer, W.A., jelesnianski, C.P., Chen, J., 1989. Hurricane storm surge forecasting. Oceans p1379–1385.

Taylor, A., Glah, B., 2008. Probabilistic guidance for hurricane storm surge. Preprints. 19th Conference on probability and statics, New Orleans, LO, USA. Mer. Meteor. Soc. 7.4 https://ams.confex.com/ams/88Annual/techprogram/paper_132793.htm.

Vickery, P.J., Masters, F.J., Powell, M.D., Wadhera, D., 2009. Hurricane hazard modelling: the past, present, and future. J. Wind Eng. Ind. Aerod. 97, 392–405. https://doi.org/10.1016/j.jweia.2009.05.005.

Walsh, K.J.E., Mcbride, J.L., Klotzbach, P.J., Balachandran, S., Camargo, S.J., Holland, G., Knutson, T.R., Kossin, J.P., Lee, T., Sobel, A., Sugi, M., 2016. Tropical cyclones and climate change. WIREs Clim. Change 7, p65–89. https://doi.org/10.1002/wcc.371, 2016.

Weather Meteorological Organization, 2017. Catalysing Innovation in Weather Science: WWRP Implementation Plan 2016-2023.

Ying, M., Knutson, T.R., Kamahori, H., Lee, T.-C., 2012. Impacts of climate change on tropical cyclones in the Western North Pacific basin. Part II: late twenty-first century projections. Trop. Cyclone Res. Rev. 1–2, p231–241. https://doi.org/10.6057/2012TCRR02.09.

Yoon, J.-J., Jun, K.-C., Shin, J.-S., Park, K.-S., 2012. Estimation of maximum typhoon intensity considering climate change scenarios and simulation of corresponding storm surge. J. Korean Soc. Mar. Environ. Eng. 15–4, p292–301. https://doi.org/10.7846/JKOSMEE.2012.15.4.292.

Yoshida, K., Sugi, M., Mizuta, R., Murakami, H., Ishii, M., 2017. Future changes in tropical cyclone activity in high-resolution large-ensemble simulations. Geophys. Res. Lett. 44, 9910–9917. https://doi.org/10/1002/2017GL075058.